
Technical Paper

Journal of the Society of
Naval Architects of Korea
Vol. 16, No. 3, September 1979

Experimental Study of Small Flapped Rudder with Rotating Cylinder and Analytical Estimation of Improvements in Ship's Maneuvering Performance with its Application

by

Keh-Sik Min

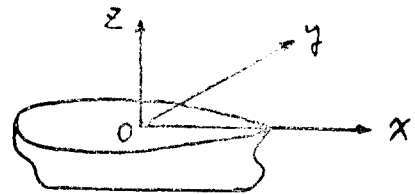
Abstract

A method of improving rudder effectiveness by applying a rotating cylinder to a rudder (so called "rotating-cylinder rudder") has been experimentally studied.

Also, the improvements in ship's maneuvering characteristics with its application has been analytically evaluated. It has been shown that this improvement is significant.

Nomenclature

a	=Aspect ratio
B	=Beam
C	=Straight-line stability criterion
C_B	=Block Coefficient
C_D	=Drag Coefficient
C_L	=Lift Coefficient
C_M	=Midship section Coefficient
C_P	=Prismatic Coefficient
C_V	=Volumetric Coefficient
D	=Steady turning diameter
H	=Draft
L	=Ship length
L_{PP}	=Length between Perpendiculars
L_{WL}	=Waterline length
m	=Hull mass coefficient
N	=Yawing moment coefficient
R	=Steady turninS radius
r	=Angular velocity
V	=Approach speed, or Ship speed
v	= y -component of V
x, y, z	=Coordinate axes fixed in the hull with origin at the center of gravity



x_G	= x -Coordinate of center of gravity
y	=Lateral hydrodynamic force coefficient
α	=Rudder deflection angle
δ	=Flap deflection angle

Subscript

R	refers to rudder
h	refers to hull without rudder
v	refers to derivatives with respect to v
γ	refers to derivatives with respect to γ

I. Introduction

Currently, great efforts are being made for the improved maneuverability of new ships. Traditionally, rudder has been used as the most effective maneuvering device. However, a conventional rudder has its own performance limit mainly due to flow separation. In fact, the study of the boundary layer

* member: Korea Research Institute of ship, Paper presented at the SNAK spring meeting held in KRIS on April 20-21, 1979.

phenomenon is one of the most important topics of marine hydrodynamics in the view points of resistance, noise, vibration, acoustics and other important problems. Maybe, one of the first men who considered the boundary layer control would be L. Prandtl (1)*. As early as in his first paper published in 1904, L. Prandtl described several experiments in which the boundary layer was controlled. Since then, numerous methods of boundary layer control have been suggested, and several methods have been developed experimentally, theoretically or both. The common purpose of these methods is to affect the whole flow in a desired direction by artificially influencing the structure of the boundary layer.

The most obvious method of avoiding separation is to attempt to prevent the formation of a boundary layer. Since a boundary layer occurs due to the difference between the velocity of the fluid and that of the solid wall, it is possible to eliminate the formation of a boundary layer by attempting to eliminate that difference, i.e. by causing the solid wall to move with the stream. The simplest way of achieving such a result involves the rotation of a circular cylinder. Figure 1 shows the flow pattern which exists about a rotating cylinder placed in stream perpendicular to its axis on the upper side, where the flow and the cylinder move in the same direction, separation is completely eliminated. Furthermore, on the lower side where the direction of fluid motion is opposite to that of the solid wall, separation is developed only incompletely. On the whole, the flow pattern which exists in this case approximates very closely the pattern of ideal flow

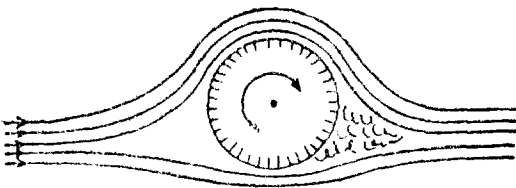


Fig. 1. Flow past a rotating cylinder

past a circular cylinder with circulation. The stream exerts a considerable force on the cylinder perpendicular to the mean flow direction, and this is sometimes referred to as the Magnus effect. Perhaps, the first application of this method is the attempts to utilize the occurrence of lift on rotating cylinders for the propulsion of ships, such as Flettner's rotor. With the exception of rotating cylinders, the idea of moving the solid wall with the stream can be realized only at the cost of very great complications as far as shapes other than cylindrical are concerned, and consequently, this method has not found much practical application. Very recently, the concept of rotating cylinder has been applied to the maneuvering system of large modern tankers, which is called "rotating cylinder rudders." Figure 2 shows the basic mechanism of boundary layer control by means of a rotating cylinder at the leading edge. This rudder system will be able to reduce the turning cycle tremendously at the low approach speed according to tests of tanker model(2). The rotating cylinder at the leading edge prevents the flow separation which usually occurs on conventional rudders at angles greater than 35 degrees. This

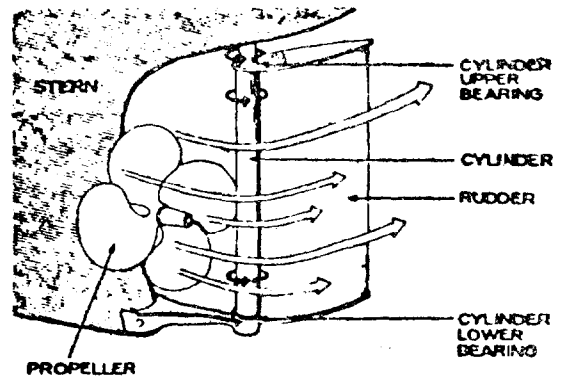


Fig. 2. Boundary Layer Control by means of Rotating Cylinder

effect makes it possible to incline the rudder at angles very close to 90 degrees to divert the propeller race through large angles. This will greatly

* Numbers in () designate numbers of references.

reduce the turning cycles and provide higher rates of turn at all ship speeds. With this concept, a model of flapped rudder with rotating cylinder was constructed, and some of its characteristics have been measured through a series of tests at the water tunnel. In this paper, the characteristics of the rudder with and without cylinder rotation will be compared and the possible improvement in ship's maneuvering performance due to its application will be estimated analytically.

II. Description of the Model

The first step in the preparation of model for this study consisted of selecting rudder type, appropriate cross-section and planform.

Originally, "all-movable single piece" type rudder (as shown in Figure 2) was considered with a rotating cylinder at the leading edge. However, it was found that this kind of model rudders had too small leading edge radius for a rotating cylinder with appreciable size to be installed with smooth overall connection and, hence, not to lose the original rudder characteristics. Therefore, "all-movable tail flap" type rudder was selected so that a cylinder could be installed at the position of the maximum thickness.

Since a rudder with rotating cylinder is relatively complicated in mechanism and much more difficult to construct than a conventional one, the overall design philosophy was set as to keep the model as simple as possible to build, while making sure that it was strong enough to stand for the various test conditions.

As a starting point, the following characteristics were considered that.

- a 1:1 aspect ratio for the simplicity
- the cylinder was to be positioned at 50% chord
- the cylinder diameter was to be same as the maximum thickness of the rudder not to protrude from the normal fair line of the chosen section from leading edge to trailing edge.

Following this idea, the NACA 16-018 section form

was selected to have the maximum thickness at the midchord (3). A rectangular planform was used for the ease of construction and later theoretical applications.

The model dimension was determined to be big enough to produce reliable data, yet small enough to successfully apply wall correction procedure.

Thus determined model characteristics are shown below.

Section form	=NACA 16-018
Planform	=Rectangular form
Aspect ratio	=1.00
Chord	=17.78cm(7.00'')
Span	=17.78cm(7.00'')
Thickness	= 4.18cm(1.25'')

This model was built by the author himself at the MIT machine shop. Among the highlights of the machining work involved in Preparing the model were the splitting and boring of the entire one-piece foil to form the skeg and flap* with room for the.

cylinder between and the contrivance of numerous precise Press-fits and alignments. This model was tested at the MIT Marine Hydrodynamics Laboratory (variable pressure water tunnel). The test procedure is discussed next chapter. Unfortunately, the test results for this model were rather disappointing and it was suspected that this disappointing results were due to too large flap. Therefore, it was decided to modify the model by reducing the flap by 1 inch. For the convenience, the original model and the modified model will be denoted by Model A and Model B, respectively. In order to smoothly connect the skeg and flap, section shape of NACA 16-021 thickness form was selected for flap portion. The characteristics of Model A and Model B are shown in Figure 3.

III. Test Procedure

As each parts of the model were prepared, they were assembled to a whole rudder and it was attached to the dynamometer base. The cylinder turns

* the forward and aft Part of the rudder.

Model A

Model B

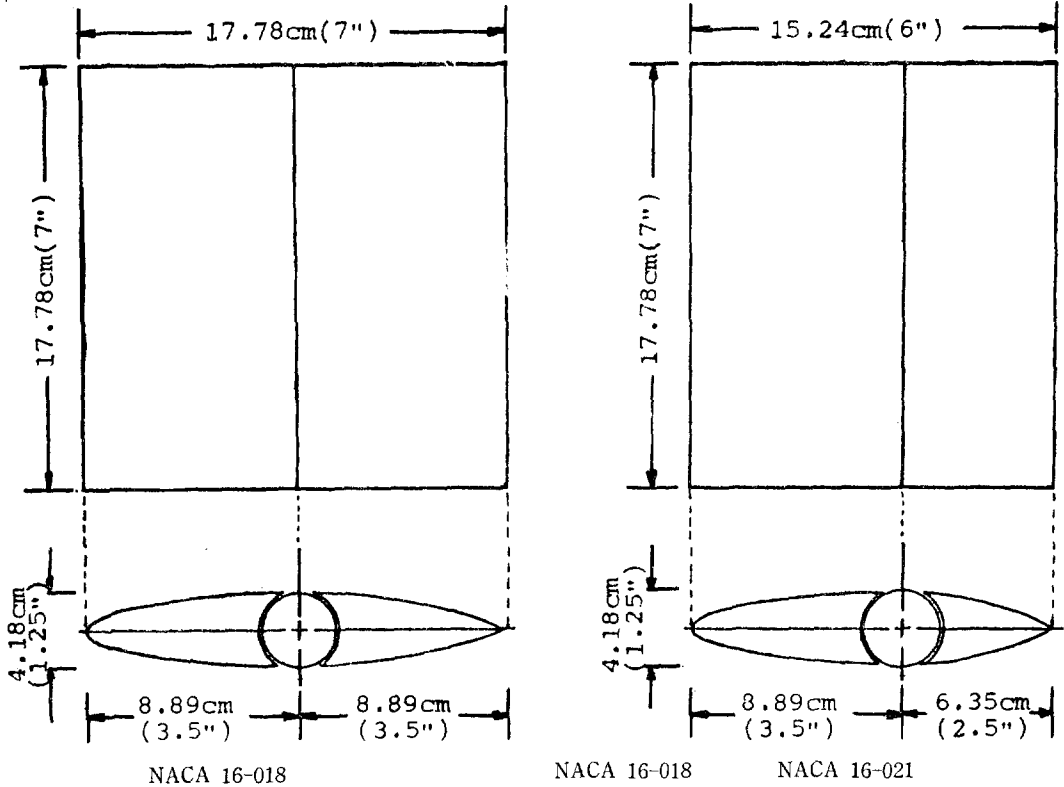


Fig. 3 Characteristics of Model A and Model B

on ball bearings mounted in the top and bottom pieces. The flap is hinged on the same axis as the cylinder with the outer surfaces of the ball bearings being used as the hinge point.

The model was designed to utilize the dynamometer system previously built for the water tunnel. This system uses six load cells to measure forces and moments generated by the body in the flow. It consists of a heavy stainless steel worm-gear base set on a tapered plexiglass plug that rotates in a matching hole in a plexiglass test section window.

A telescope mounted on top that focuses on a wall-mounted scale permits accurate, repeatable angle of attack adjustments.

The model was rigidly attached to a base plate and shaft arrangement of its own. The 3.81 cm ($1\frac{1}{2}$ ") stainless steel shaft passes out from the

tunnel section through a seal to be rigidly clamped to the floating structure of the dynamometer. This floating structure is then connected to the dynamometer base (described above) by a set of Lebow Model 3345 strain gage load cells.

The load cells are attached through slender, high-strength steel flexures that provide as close as possible to ideal pin-end support. These load cells are electrically connected to Lebow Model 66 digital strain indicators. The resulting calibration and operation of this dynamometer system have been very satisfactory.

Power for the cylinder was supplied via shaft from an electric motor source external to the tunnel.

The electric motor system to drive the cylinder was mounted on the rigid platform of the dynamometer. Thus it does not affect the force or moment

readings at all. It drives the cylinder by means of a timing belt assembly and a long shaft that passes through a hole that was drilled in the 3.81cm(11/2) dynamometer attachment shaft mentioned before. Bench testing revealed that with the entire unit, foil, dynamometer, and power system assembled the cylinder could be driven in excess of 7,000rpm, and the whole assembly was as rigid as expected. The ratio of the tangential speed of the cylinder to the free stream speed (which may be the most important quantity) was decided as the values of 0.75, 1.0, 1.5 and 2.0 with a zero cylinder rpm run as a reference.

The above ratios correspond to cylinder rpm's of 2062, 2750, 4125 and 5500, respectively. This rpm was measured with a Hewlett-Packard counter and magnetic pick-up reading off a sixty tooth gear. Although the flap could deflect up to 50 degrees, test was done at zero and 40 degrees of flap deflection due to the long required time to finish each condition. The flap was positively fixed at each angle of deflection to the mounting plate by two Allen bolts. Tests were conducted at each of the two flap deflections for each of the five cylinder RPM values and for the complete range of angles of attack as constrained by the data reduction program.

IV. Test Results

In order to present the test results, a sign convention has been adopted as shown in Figure 4.

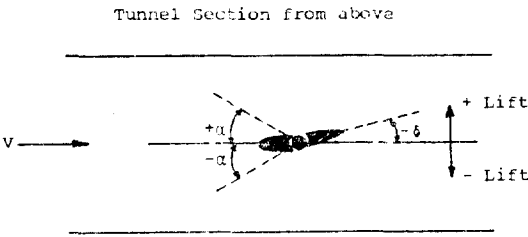


Fig.4 Sign Convention

As Previously mentioned, raw test data were reduced to detail hydrodynamic properties through the data reduction Program. This program includes the corrections for the load cell readings for zero

drift, for the temperature effect on the flow speed and for the tunnel wall effect. One sample output is shown in Table 1. However, the entire computer output will not be included here due to limited space.

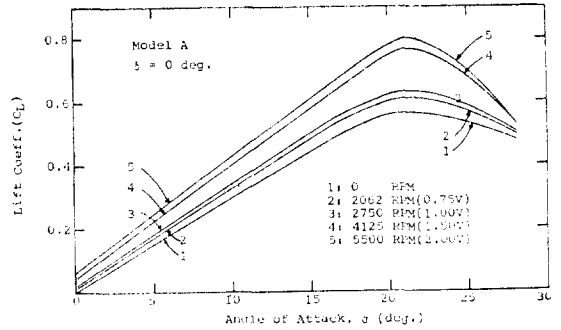


Fig. 5. Lift Coefficient

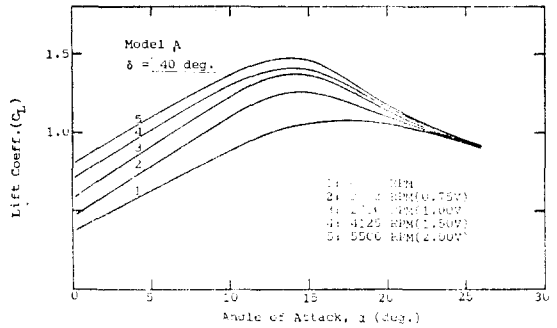


Fig. 6. Lift Coefficient

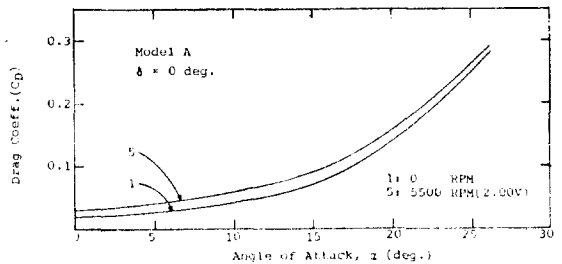


Fig. 7. Drag Coefficient

Table 1. Sample Computer Output of Hydrodynamic Characteristics

Model B Delta 0 deg. 0 RPM

PRIOR DATA CORRECTED FOR TUNNEL INTERFERENCE

ALPHA	CL	CD	CM	CPL	CY	L/D	CMF	RN*10 **6	CLSO
0.00	0.000	0.0405	0.0	-0.675	-0.026	0.005	0.0	0.948	0.0000
2.03	0.033	0.0402	0.0333	-0.675	-0.026	0.815	0.0	0.948	0.0011
4.06	0.060	0.0409	0.0665	-0.675	-0.026	1.458	0.0	0.948	0.0036
6.10	0.104	0.0443	0.1001	-0.675	-0.026	2.345	0.0	0.947	0.0108
8.15	0.153	0.0506	0.1311	-0.675	-0.026	3.017	0.0	0.948	0.0233
10.21	0.213	0.0606	0.1610	-0.675	-0.026	3.522	0.0	0.946	0.0455
12.27	0.285	0.0748	0.1923	-0.675	-0.026	3.807	0.0	0.947	0.0810
14.34	0.354	0.0901	0.2206	-0.675	-0.026	3.935	0.0	0.949	0.1255
16.41	0.431	0.1092	0.2452	-0.675	-0.026	3.950	0.0	0.947	0.1861
18.47	0.497	0.1296	0.2641	-0.675	-0.026	3.838	0.0	0.948	0.2475
20.54	0.568	0.1525	0.2880	-0.675	-0.026	3.724	0.0	5.947	0.3226
22.58	0.609	0.1730	0.3010	-0.670	-0.026	3.520	0.0	0.948	0.3707
24.51	0.538	0.3256	0.2301	-0.675	-0.026	1.638	0.0	0.946	0.2896
-2.03	-0.035	0.0413	-0.0334	-0.675	-0.026	-0.845	0.0	0.946	0.0012
-4.06	-0.062	0.0433	-0.0648	-0.675	-0.026	-1.432	0.0	0.946	0.0038
-6.10	-0.099	0.0480	-0.0965	-0.675	-0.026	-2.064	0.0	0.945	0.0098
-8.17	-0.171	0.0544	-0.1272	-0.675	-0.026	-3.147	0.0	0.948	0.0293
-10.23	-0.245	0.0636	-0.1609	-0.675	-0.026	-3.849	0.0	0.947	0.0599
-12.30	-0.317	0.0729	-0.1889	-0.675	-0.026	-4.344	0.0	0.945	0.1004
-14.38	-0.397	0.0855	-0.2207	-0.675	-0.026	-4.643	0.0	0.945	0.1576
16.44	-0.460	0.1008	-0.2449	-0.675	-0.026	-4.565	0.0	0.947	0.2118
-18.50	-0.531	0.1216	-0.2658	-0.675	-0.026	-4.368	0.0	0.945	0.2820
-20.55	-0.584	0.1384	-0.2853	-0.675	-0.026	-4.215	0.0	0.945	0.3405
-22.60	-0.630	0.1610	-0.3000	-0.675	-0.026	-3.912	0.0	0.947	0.3969
-24.38	-0.396	0.3051	-0.1885	-0.675	-0.026	-1.300	0.0	0.946	0.1572

ALPHA=0 D/DALPHA D/DALPHA**2
 CL COEFFS -0.008112 0.023355
 CD COEFFS 0.038421 -0.000001 0.000234 DYCOR= -1.11480
 DCD/DCL**2= 0.429587

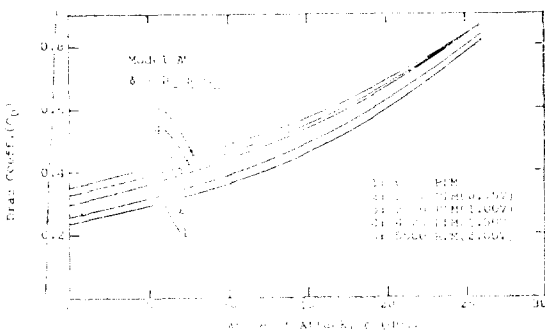


Fig. 8. Drag Coefficient

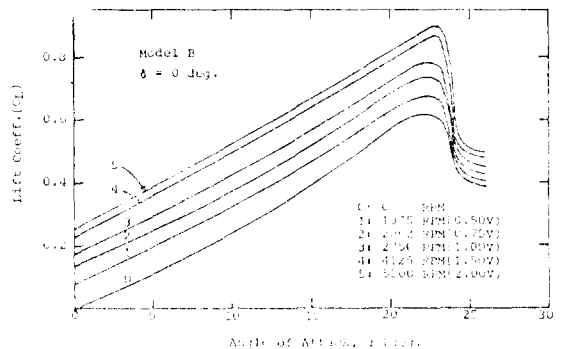


Fig. 9. Lift Coefficient

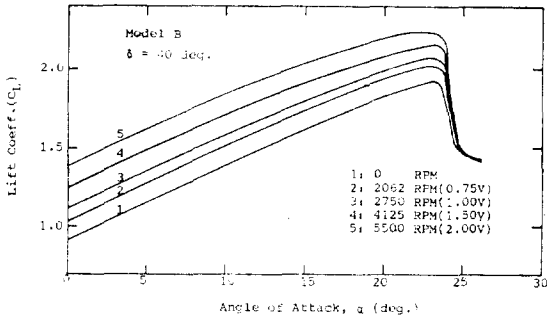


Fig. 10. Lift Coefficient

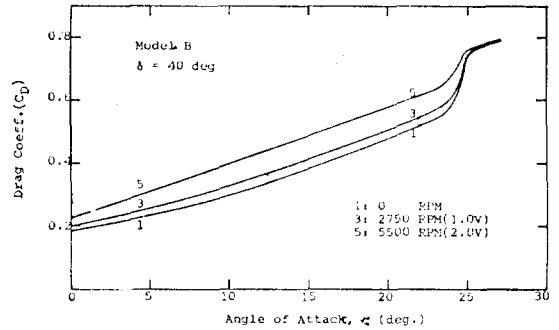


Fig. 12. Drag Coefficient

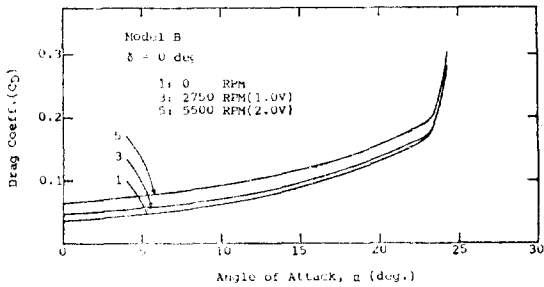


Fig. 11. Drag Coefficient

Instead, some performance characteristics from the output will be summarized in the form of Table and Figure. The lift and drag coefficients for 0 degree and 40 degrees flap deflections for Model A and B are shown in Figure 5 to 12. Also, comparisons of some typical characteristics between Model A and Model B are shown in Table 2, and Figures 13 and 14.

Table 2. Comparison of Principal Hydrodynamic Characteristics between Model A and Model B
Flap Deflection, $\delta=0$ deg.

Model RPM Characteristics	Model A					Model B				
	0	2062	2750	4125	5500	0	2062	2750	4125	5500
(C_L) max	0.604	0.669	0.724	0.811	0.850	0.630	0.752	0.809	0.882	0.904
α at (C_L) max	20.0	22.9	22.9	25.0	25.0	22.6	22.7	22.8	22.8	22.9
(C_L) at $\alpha=0$	0.0	0.025	0.047	0.073	0.090	0.0	0.152	0.181	0.238	0.261
C_D at (C_L) max	0.146	0.172	0.178	0.218	0.223	0.161	0.162	0.164	0.181	0.185
α at stall	22.0	22.0	21.0	21.0	21.0	22.6	22.7	22.8	22.8	22.9

Flap Deflection, $\delta=40$ deg.

Model RPM Characteristics	Model A					Model B				
	0	2062	2750	4125	5500	0	2062	2750	4125	5500
(C_L) max	1.200	1.363	1.440	1.480	1.505	1.440	1.530	1.580	1.660	1.730
α at (C_L) max	21.5	20.0	20.0	20.0	20.0	23.3	23.4	23.5	22.8	22.8
(C_L) at $\alpha=0$	0.500	0.711	0.890	0.993	1.003	0.411	0.530	0.610	0.740	0.870
C_D at (C_L) max	0.586	0.584	0.630	0.646	0.658	0.548	0.568	0.567	0.594	0.606
α at stall	22.0	22.0	21.0	21.0	21.0	23.3	23.4	23.5	22.8	22.8

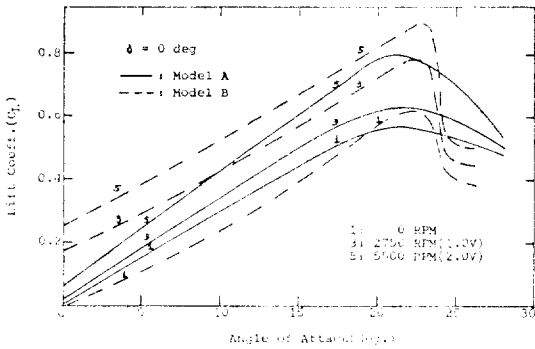


Fig. 13. Comprison of Lift Coefficient

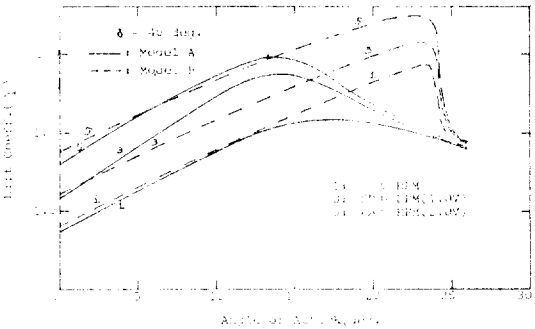


Fig. 14. Comparison of Lift Coefficient

V. Application to Tanker Model

In order to estimate the improvement in maneuvering performance of a ship with its application, a large modern tanker has been selected as a model. The characteristics of the model ship are shown in Table 3 and Fig. 15(4). Recently, certain definitive maneuvers have been devised to demonstrate a ship's maneuverability and accepted by the naval architects.

The definitive maneuvers employed for both surface ships and submarines are.

1. Spiral maneuver
2. zig-zag maneuver
3. turning maneuver

Essentially, these maneuvers establish the basic stability and control characteristics of a ship independent of its operator. Although all three maneuvers are important for both commercial and naval ships, only the steady turning maneuver will be considered quantitatively, because it has traditionally received the most attention in ship maneuverability and because its analytical treatment can be done more readily. Both linear and nonlinear theories are available. For the conventional displacement type ships, the steady turning diameter is usually order of several ship lengths even at the maximum rudder deflection. Therefore, the linear theory is quite adequate and will be utilized.

Table 3. Characteristics of Model Ship (without Bulb)

Hull Form		Series 60 (8)
LPP,	m	307.00
LWL,	m	309.45
B(molded),	m	44.50
H(molded),	m	13.00
Volume,	m ³	123,800
Displacement,*	tons	127,000
C_B^*		0.697
C_P^*		0.707
C_M^*		0.985
$C_V \times 10^{34}$		4.177

*based on LPP

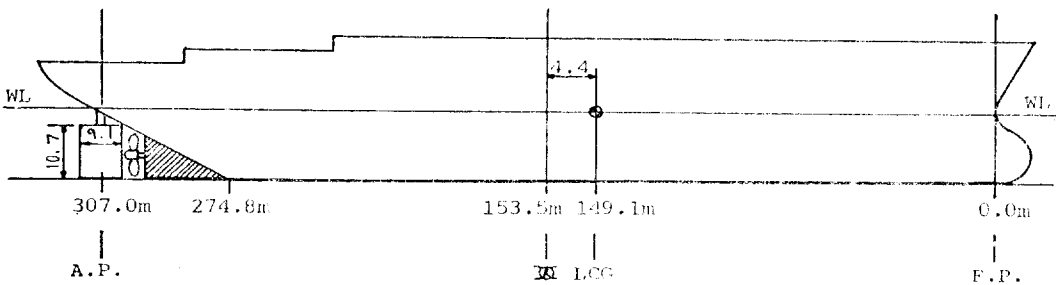


Fig. 15. Sketch of Model Ship profile

Since linear theory is applicable only to stable ships, the motion stability (straight-line stability) should be checked first. The stability criterion, C , may be expressed as (5).

$$C = Y_v'(Nr' - m'x_G') - N_v'(Y_r' - m') > 0$$

and it will be shown later (Table 4) that this criterion has been satisfied. In linear theory, ship's

steady turning radius is expressed as (5)

$$R = \frac{L}{\alpha} \cdot \frac{Y_v'(Nr' - m'x_G') - N_v'(Y_r' - m')}{Y_v'N\alpha' - N_v'Y\alpha'}$$

However, the above equation is the expression for the ship with a conventional rudder (or rudders) and cannot be applied directly. In order to utilize the rest results for the rudder with a rotating

Table 4. Summary of Hydrodynamic Derivatives and Related Nondimensional Quantities
PNA's Notation
Flap deflection, $\delta=40$ deg.

Derivatives $\times 10^5$	α (deg)	Hull	Skeg	Rudder			Total
				0 RPM	2750 RPM	5500 RPM	
Y_v'		-607	-461	-198			-1266
Y_r'		-9	221	104			316
N_v'		-581	221	104			-256
N_r'		-86	-106	-55			-247
$\bar{Y}_R'^*$	0			42	63	91	
	5			68	88	116	
	10			92	112	139	
	15			115	135	159	
	20			138	154	176	
$\bar{N}_R'^*$	0			-22	-33	-48	
	5			-36	-46	-61	
	10			-48	-59	-73	
	15			-60	-71	-84	
	20			-72	-81	-93	
m'				369			
x_G'				0			
C				3.11			

* determined from experiment

Table 5. Steady Turning Characteristics of the Tanker Model
Rudder Model B
Flap Deflection, $\delta=40$ deg.
Approach Speed=23.5 knots

α (deg.)	Steady Turning Diameter (m)			Turning Diameter $\left(\frac{D}{L}\right)$ Ship Length		
	0 RPM	2750 RPM	5,500 RPM	0 RPM	2,750 RPM	5,500 RPM
0	4,757	3,171	2,185	15.49	10.33	7.12
5	2,915	2,273	1,717	9.50	7.41	5.60
10	2,178	1,777	1,435	7.1	5.79	4.67
15	1,742	1,476	1,249	5.68	4.81	4.07
20	1,452	1,294	1,127	4.73	4.21	3.67

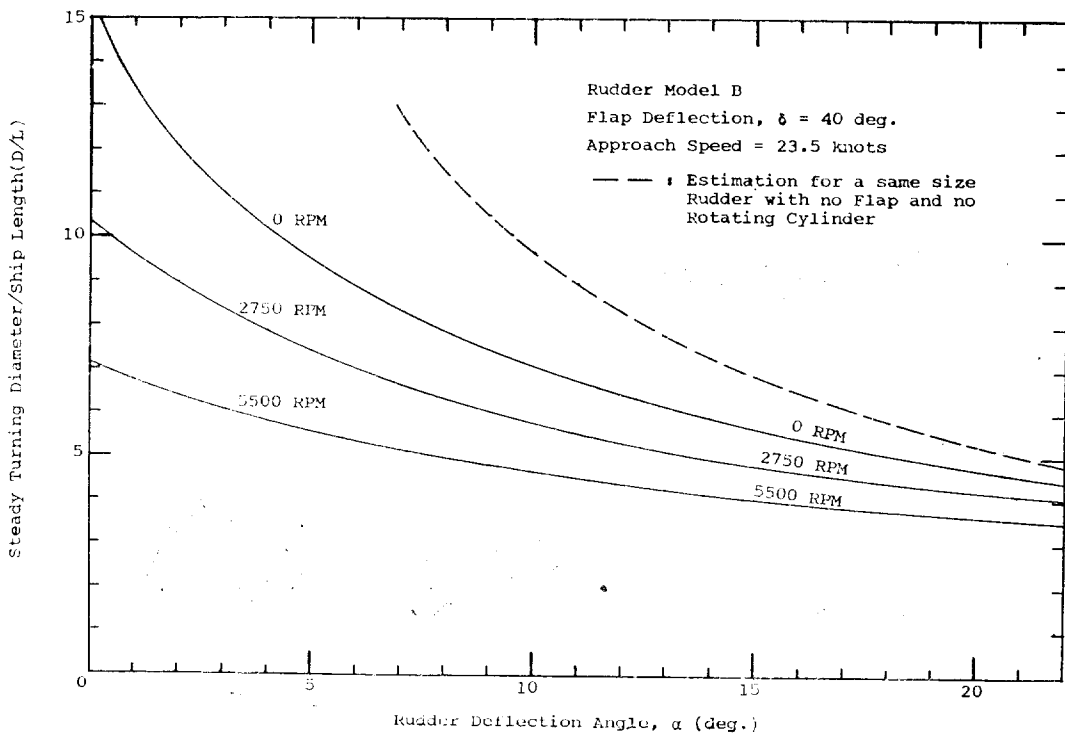


Fig. 16. Steady Turning Characteristics of the Tanker Model

cylinder, therefore, it is necessary to slightly modify the above expression as,

$$D=2L \cdot \frac{Y_v'(N_r' - m'x_G') - N_v'(Y_r' - m')}{Y_v'\bar{N}_R' - N_v'\bar{Y}_R'}$$

Where,

Y_R' =nondimensional lateral force of rudder

\bar{N}_R' =nondimensional yaw moment due to lateral force of rudder

The hydrodynamic derivatives for the tanker model have been analytically estimated mostly based on the theory discussed in reference 6 and summarized in Table 4. A typical example for the detailed procedures of estimation is shown in reference 7. With the above modified equation and with the hydrodynamic derivatives summarized in Table 4, the steady turning characteristics of the ship can be calculated, and are Presented in Table 5 and Figure 16.

VI. Discussions and Conclusions

Before making any conclusion, some effects on

the rudder Performance should be discussed first.

(1) Effect of Reynolds Number

Generally, the performance of a lifting surface is not much affected by Reynolds number, that is, lift and drag for any lifting surfaces of given shape are Primarily dependent on the angle of attack as long as no separation or no stall occur. However, the effect of Reynolds number on the maximum lift and stall angle is serious. Free-stream rudder tests indicate qualitatively that the higher the Reynolds number is, the larger the angle of attack at which stall occurs and, hance, the greater the maximum attainable lift is.

(2) Scale Effect

Reynolds number for the model rudder (6×10^5 at corresponding model speed to ship speed) is much less than that for the full scale rudder (1×10^8 for the ship speed of 23.5 Knots).

At low Reynolds number, the flow about a model rudder may be laminar than turbulent. Since laminar flow is much more susceptible to separation than is

turbulent flow, this may be a factor in inducing premature stall in model tests of rudder.

(3) Effect of Aspect ratio

There is an inverse relation between the aspect ratio and the stall angle, that is, the higher the aspect ratio is, the smaller the angle of attack at which stall occurs is.

With the above preliminary discussions, and from the analysis and application of test results, the following conclusions are made:

1. Higher lift coefficient always occurs at higher cylinder rpm for all flap angles.
2. In general, increasing cylinder rpm increases the Lift/Drag ratio and thereby increase the efficiency of the rudder at the maximum lift point.
3. The effect of rotation of cylinder is little for zero flap deflection angle and becomes more and more significant with increasing flap deflection angle. This result is quite obvious because large cylinder area can be exposed to the fluid with higher flap deflection angle.
4. It is disappointing that increasing cylinder rpm has negligible effect on the stall angle. This situation may be explained that this system can affect the flow pattern after cylinder, but may not be able to considerably influence the flow characteristics before the cylinder.
5. In most cases, model B has higher lift and lower drag coefficients than Model A. This is particularly true for larger flap deflection. Clearly, the effect of too large flap is unfavorable on hydrodynamic characteristics. There must be a optimum flap size. However, it is not possible to determine the optimum flap size with this single study.
6. As shown in Fig. 16, the steady turning diameter of a ship can be reduced remarkably with the application of the rotating cylinder rudder, and this improvement is more significant at lower rudder deflection. The actual improvement in maneuvering performance of a full scale ship is expected to be

greater than that Predicted by this study due to reasons of previous discussions and others. Since the required power in rotating the cylinder is quite negligible compared with that of ship propulsion, the application of a rotating cylinder is well justified. The complication in mechanism of steering system and structural strength are other problems.

Acknowledgement

The author wishes to express his appreciation to Mr. Ki-Sup Kim for his help in Preparing the figures. Also, thanks are extended to Miss Myung-Ja Lee for her typing the manuscript. Both of them are members of the Hydrodynamics Research Department of KRIS.

References

- (1) A. Betz, History of boundary layer control research in Germany. In *"Boundary layer and flow control"* (G.V. Iachmann, ed.), Vol. 1, 1-20, London, 1961.
- (2) *Ocean Industry*, July, 1973.
- (3) I.H. Abott and A.E. Von Doenhoff, *Theory of Wing Sections*, Dover Publications, New York.
- (4) Ingal shipbuilding, 125,000 ton class LNG tanker, Hull forms and performance characteristics, Preliminary design drawing No. N44 DG 1-10, 1972.
- (5) P.N.A., 1967 Edition, SNAME.
- (6) W.R. Jacobs, Estimation of stability derivatives and indices of various ship forms, and comparison with experimental results, *Trans.*, SNAME, 1966.
- (7) K. Min, 571 Project Ship, Study of Maneuvering Characteristics (Part 1), *Korea Research Institute of Ship and Ocean*, August, 1977.
- (8) F.H. Todd, Series 60 Methodical experiments with model of single-screw merchant ship, *DTMB Report 1712*, July 1963.

科學技術者倫理要綱

現代的 國家發展에 미치는 科學技術者의 役割의 重要性에 비추어 우리들 科學技術者는 우리들의 行動의 指針이 될 倫理要綱을 아래와 같이 制定하고 힘써 이를 지킴으로써 祖國의 近代化에 이바지할 것을 깊이 銘心한다.

1. 우리들 科學技術者는 모든 일을 最大限으로 誠實하고 公正하게 處理하여야 한다.
2. 우리들 科學技術者는 恒常 專門家로서의 權威를維持하도록 努力하며 自己가 所屬하는 職場 또는 團體의 名譽를 昂揚하여야 한다.
3. 우리들 科學技術者는 法律과 公共福利에 反하는 어떠한 職分에도 從事하여서는 안되며, 의아스러운 企業體에 自己의 名稱을 빌려주는 것을 拒絕하여야 한다.
4. 우리들 科學技術者는 依賴人이나 雇傭主로부터 取得 또는 그로 因해 얻어진 科學資料나 情報에 對하여는 秘密을 지켜야 한다. 또는 他人의 資料情報을 引用할 때는 그 出處를 밝혀야 한다.
5. 우리들 科學技術者는 誇張 및 無限한 發言과 非權威的 또 眩惑的 宣傳을 삼가야 하며 또 이를 制止하여야 한다. 特히 他人의 利害에 關係되는 評價報告 및 發言에는 慎重을 期하여야 한다.
6. 우리들 科學技術者는 어떠한 研究가 그 依賴者에게 利益이 되지 않음을 아는 경우에는 이를 미리 알리지 아니하고는 어떠한 報酬를 위한 研究도 擔當하지 않는다.
7. 우리들 科學技術者는 祖國의 科學技術의 發展을 위하여 最大限으로 奉仕精神을 發揮하여야 하며 또한 이를 위한 應分의 物質的 協助을 아껴서는 안된다.